

Phenol decomposition under sunlight using a sonochemically synthesized CdSe/TiO₂ nanocatalyst

Mohammad Saleh Ghodrati · Mohammad Haghghi · Jafar Sadegh Soltan Mohamdzadeh · Behzad Pourabas · Ehsan Pipelzadeh

Received: 13 October 2010/Accepted: 4 June 2011/Published online: 24 June 2011
© Akadémiai Kiadó, Budapest, Hungary 2011

Abstract Ultrasound energy has been successfully employed to synthesize CdSe/TiO₂ nanocatalysts for the photocatalytic degradation of phenol under solar light irradiation. The photocatalytic performance test was carried out using TiO₂ as well as synthesized CdSe/TiO₂ nanocatalysts. Nanocatalyst characterization was accomplished using XRD, SEM, FTIR, BET and UV-vis spectroscopy. It was shown that the synthesized nanocatalysts have crystal characteristics and are in nano-scale size range. The coupled nanocatalyst has shown a shift in the absorption spectrum from the UV range to the visible range. The results of photocatalytic tests showed that the CdSe/TiO₂ coupled nanocatalyst could remove phenol from wastewater under solar light irradiation, while TiO₂ did not have enough activity in this process. It is also shown that the CdSe nanoparticles act as photosensitizers, not only extending the spectral response of TiO₂ to the visible region but also reducing the electron–hole recombination. Furthermore, the CdSe/TiO₂ synthesized samples

M. S. Ghodrati · M. Haghghi (✉) · J. S. Soltan Mohamdzadeh · E. Pipelzadeh
Chemical Engineering Faculty, Sahand University of Technology, Sahand New Town,
P. O. Box 51335-1996, Tabriz, Iran
e-mail: haghghi@sut.ac.ir
URL: <http://rcrc.sut.ac.ir>

M. S. Ghodrati · M. Haghghi · J. S. Soltan Mohamdzadeh · E. Pipelzadeh
Reactor and Catalysis Research Center (RCRC), Sahand University of Technology,
Sahand New Town, P. O. Box 51335-1996, Tabriz, Iran

M. Haghghi · B. Pourabas · E. Pipelzadeh
Nanostructure Material Research Center (NMRC), Sahand University of Technology,
Sahand New Town, P. O. Box 51335-1996, Tabriz, Iran

J. S. Soltan Mohamdzadeh
Department of Chemical Engineering, University of Saskatchewan, 57 Campus Drive,
Saskatoon, SK S7N 5A9, Canada

provided more photomineralization efficiency than that of TiO₂ in terms of total organic carbon analysis.

Keywords Phenol decomposition · Titanium dioxide · Cadmium selenide · Nanocatalyst · Sonochemistry · Photocatalytic · Sunlight

Introduction

Phenolic compounds are widely used in chemical industries and daily life as solvents and byproducts. Mainly because of their high stability, high toxicity and carcinogenic character, they have caused considerable damage and threat to the ecosystem in water bodies and human health [1]. Methods to eliminate phenolic compounds effectively from wastewater have been extensively reported. The conventional wastewater treatment techniques include activated carbon adsorption, chemical oxidation and biological digestion. Among them, photocatalytic degradation assisted by titanium dioxide under ultraviolet is one of the techniques widely studied [2–5]. Many researchers have focused on types and modification of the existing catalysts [6–8], the photocatalytic principles, the factors influencing photocatalytic reaction rate [7] and the reaction kinetics [2, 5, 6].

The photocatalytic degradation of phenolic compounds in aqueous medium has several advantages over conventional oxidation processes. These are the complete mineralization of pollutant, the utilization of near UV light and no needs of chemicals. The possible extents of the technique concern the irradiation source and the physical state of the pollutant. Recently, some reports have pointed out that the degradation of organic compounds is induced by visible light when the nanoparticles are incorporated with other semiconductors or metals. Therefore, the great interest is to use solar light, which is free and inexhaustible [6].

Several semiconductors with photocatalytic properties have been developed. The most commonly used semiconductors for waste degradation are TiO₂ [9], ZnO [10] and CdSe [6]. Most studies on photoassisted decomposition of chlorinated organic compounds used TiO₂ as a model photocatalyst because of the photooxidation efficiency and stability of TiO₂ under illumination in aqueous environments [11]. A dosage of 2–5 g/l TiO₂ irradiated by near-UV light (with wavelength near 400 nm) can decompose chlorophenol to inorganic carbon in about 350 min without consuming any chemicals and generating sludge [11, 12]. TiO₂ has also been employed to investigate photodegradation of various organic pollutants such as *p*-coumaric acid [13] and 2-phenylphenol [10]. CdSe undergoes photo corrosion when illuminated with ultraviolet light which is prohibited when coupled with TiO₂ [14]. Shih-Chen Lo et al. used coupled CdSe/TiO₂ for degradation of 4-chlorophenol under visible light irradiation [15]. Later on, Wingkei Ho et al. employed coupled CdSe/TiO₂ for the same treatment under the visible light emitted from a 300 W tungsten halogen lamp with a 400 nm cut off filter [6].

One of the drawbacks of using TiO₂ and advanced oxidation processes for water remediation is its UV range dependence thus making only a small amount of sunlight spectrum useful for the photocatalytic degradation of organic pollutants. In

this work, an ultrasonic assisted method was developed for syntheses of a CdSe/TiO₂ nanocatalysts with crystal structures at different precursor ratios. The catalysts were used for the photodegradation of phenol under illumination of sunlight. The aim of this work was to determine an optimum ratio for the CdSe to TiO₂ nanoparticles synthesized via the sonochemical approach.

Materials and methods

Analytical grade chemicals were used in all experiments in this work. Phenol was purchased from Merck Co. with a purity of >99%, while TiO₂ was purchased from Degussa (Degussa P25). For all tests, doubly distilled water was used. The experimental work consists of preparation of CdSe/TiO₂, characterization of coupled CdSe/TiO₂ and photodegradation of phenol using the commercially available TiO₂ and synthesized coupled CdSe/TiO₂.

Nanocatalysts preparation and procedures

CdSe synthesis

The schematic flow chart for the ultrasonic assisted preparation steps of CdSe is shown in Fig. 1. Equimolar amounts of sodium hydrogen selenite and sodium hydroxide were mixed in 50 mL of distilled water. The solution was stirred and heated at 100 °C until it was completely dried. The resulting Na₂SeO₃ was further milled and diluted in distilled water. In a 250 mL conical flask, the synthesized sodium selenite (0.0025 mol) was primarily added to 5 mL of 1 M hydrazine hydrate (N₂H₄·H₂O) solution. Cadmium nitrate (Cd(NO₃)₂, 0.005 mol, 1 M) was pre-dissolved in 3 mL of aqueous ammonium NH₃·H₂O and intermixed with diluted

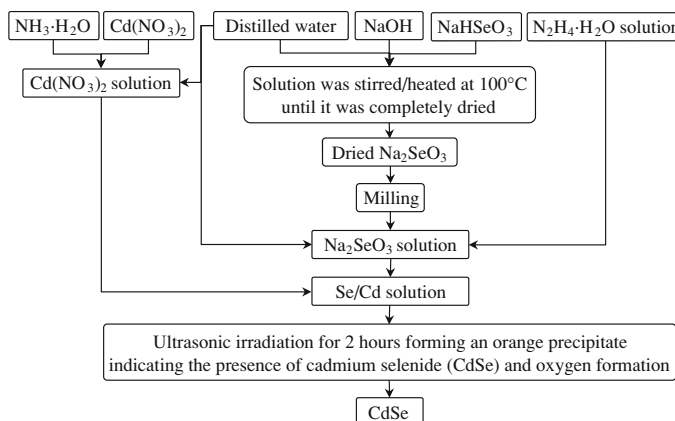
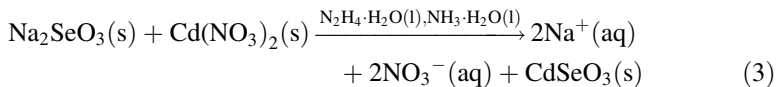
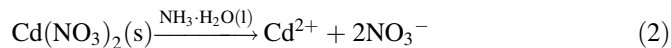
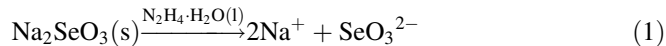


Fig. 1 Schematic flow chart for the ultrasonic assisted preparation steps of CdSe

solution of the synthesized sodium selenite. The mixture was exposed to ultrasonic irradiation for 2 h forming an orange precipitate indicating the presence of cadmium selenide (CdSe). Eq. 1–4 show the suggested reactions that lead to the formation of cadmium selenide, CdSe.

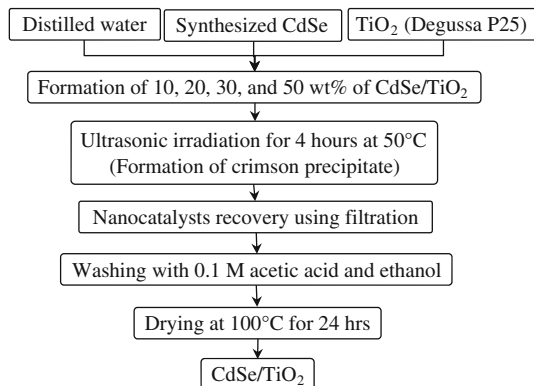


As shown, sodium selenide is dissociated into sodium and selenite ions in the presence of hydrazine hydrate, while cadmium and nitrate ions are formed because of cadmium nitrate dissociation in the presence of aqueous ammonium solution. Further exposure to ultrasonic irradiation resulted in cadmium selenide (CdSe) and oxygen formation.

CdSe/TiO₂ synthesis

The schematic flow chart for the ultrasonic assisted addition of CdSe to TiO₂ is illustrated in Fig. 2. The nanocomposites were prepared as in an earlier Ref. [6]. Different amounts of commercially available TiO₂ (Degussa P25) were added to the prepared CdSe forming 10, 20, 30, and 50 wt% of CdSe/TiO₂. The nanocatalysts were prepared by a fixed amount of the CdSe and the addition of different amounts of TiO₂. The mixture was further treated with a 4-h ultrasonic irradiation of the TiO₂ and CdSe mixture using a bath sonicator at 50 °C forming a crimson precipitate. The nanocatalysts were recovered using a paper filter, and washed with

Fig. 2 Schematic flow chart for the ultrasonic assisted addition of CdSe to TiO₂



0.1 M acetic acid and ethanol consecutively. Further drying was performed at 100 °C using an oven.

Nanocatalyst characterization

UV-vis spectroscopy (250–800 nm) was performed with a Spectronic 401—MiltonRoy instrument to account for the absorption characteristics of the photocatalysts. For crystallographic analysis of the synthesized nanocatalysts, XRD patterns were recorded using TW3710 Philips X'Pert diffractometer using CuK α radiation ($\lambda = 1.54 \text{ \AA}$). Data were collected in the range of $20^\circ \leq 2\theta \leq 60$ with a 0.02° sweep rate at 40 kV 30 mA. Morphological studies were conducted using a scanning electron microscope (SEM, Viga II, 3×10^5 , USA). FTIR analyses were performed using a Unicam Matteson 4000 instrument to account for adsorbed compounds on the synthesized nanocatalysts from the reaction media and surrounding atmosphere. The specific surface area (BET) of nanocomposites was characterized by nitrogen adsorption and desorption isotherms obtained at -196°C using a Quantachrom apparatus. Total organic carbon (TOC) analyses were performed using a scalar formacs^{HT} TOC/TN analyzer to account for the organic carbon present in the course of photo-degradation of phenol.

Phenol photocatalytic decomposition tests

Phenol was added as an organic contamination and its course of photodecomposition was taken as a test for photocatalytic performance of the synthesized nanocatalysts and that of the commercially available Degussa TiO₂ under illumination of sunlight light July, Tabriz 38 North, 46 East (East Azarbayjan) with an average intensity 2.960 W/cm² measured at 365 nm. 35 ppm of phenol was added to a suspension of 0.8 g/L photocatalyst in a 250 mL conical flask. The flask was equipped with an oxygen intake to bubble oxygen into the photoreactor at the rate of 15 mL/min. The photoreactor was placed in a water jacket keeping the reaction media at 25 °C. Samples were taken at 15 min intervals from the reaction media and filtered using a 0.45 μm filter to form a clear solution. Further investigation of photocatalytic performance was conducted using a Philips UV-vis spectroscopy, indicating the degree of phenol degradation having prepared standard phenol solutions (1–100 ppm) concentrations and calibration curve. Phenol shows an intense absorption at 269.4 nm in UV and the intensity of this peak changes with concentration. The experiments were repeated for three times revealing its repeatability using fresh and used photocatalysts.

Prior to the photocatalytic examinations, two preliminary tests were carried out. In order to check the extent of phenol adsorption on nanocatalysts, the synthesized nanocatalysts were subjected to phenolic media for 40 min in the dark. The adsorption experiment revealed no detectable change of phenol concentration suggesting that phenol had not been adsorbed on TiO₂ surface in the dark. No photocatalytic activity was observed when phenol was added to both TiO₂ and the synthesized CdSe/TiO₂ nanocatalyst mixture subjected to dark conditions. This can be addressed by crucial role of photo illumination.

Results and discussion

XRD, SEM, FTIR, BET and UV-vis spectroscopy analysis were performed to study the crystalline structure phases, surface properties and absorption spectrum of the synthesized nanocatalysts non-modified Degussa TiO₂. Furthermore, photodecomposition analysis is performed under sunlight irradiation where phenol was added as an organic pollutant.

Nanocatalyst characterization

Crystallographic studies

Fig. 3 shows the XRD pattern of synthesized CdSe (a) and commercial TiO₂ (b) as well as ultrasonically synthesized nanocatalyst CdSe/TiO₂ containing 10, 20, 30 and 50 wt% of CdSe (c–f). As it can be seen from the crystallographic studies, the ultrasonically synthesized CdSe has a hexagonal crystal. The CdSe incorporated with TiO₂ shows both the anatase and rutile phases corresponding to TiO₂ nanoparticles and the hexagonal phase of the CdSe.

Absorption spectroscopy

Fig. 4 shows the UV–vis absorption spectra of TiO₂ (a) and that of the synthesized CdSe/TiO₂ nanocatalyst (b–e). The results show an increase in the absorption range from UV regions (400 nm) to visible region. The studies have shown a proportional increase in the visible region absorption as the CdSe content is increased. Using the Planck equation, $E = hv$, the band gap energy of TiO₂ and that of the CdSe/TiO₂ (20 wt%) nanocatalyst are calculated to be 3.1 and 2 eV in accordance to the critical wavelengths. These are close to 3.2 and 1.7 eV as reported in the literature for TiO₂ and that of the CdSe/TiO₂ (20 wt%) nanocatalyst, respectively [16].

FTIR analysis

Fig. 5 shows FTIR results obtained for non-modified Degussa TiO₂ (a) and the synthesized nanocatalyst with 20 wt% CdSe (b). All the spectra show one broad band near 3400 cm⁻¹ which correspond to surface-adsorbed water and hydroxyl groups [17, 18]. The peak at 1630 cm⁻¹ is due to O–H bending of adsorbed water molecules [19]. The peaks over when 400–1250 cm⁻¹ are characteristic of the O–Ti–O network. The peaks at 1000–1500 cm⁻¹ is due to the existence of different bonds in both CdSe and TiO₂ in the nanocatalyst. The peak centered at about 1384 cm⁻¹ corresponds to the C–O stretch bond present in residual organics [20]. This peak is a result of the adsorbed organic material that is incorporated into the titanium structure.

Morphological studies

Fig. 6 illustrates the SEM micrographs of the TiO₂ (a) and that of synthesized CdSe/TiO₂ (20 wt%) nanocatalyst (b). The micrographs reflect a morphology

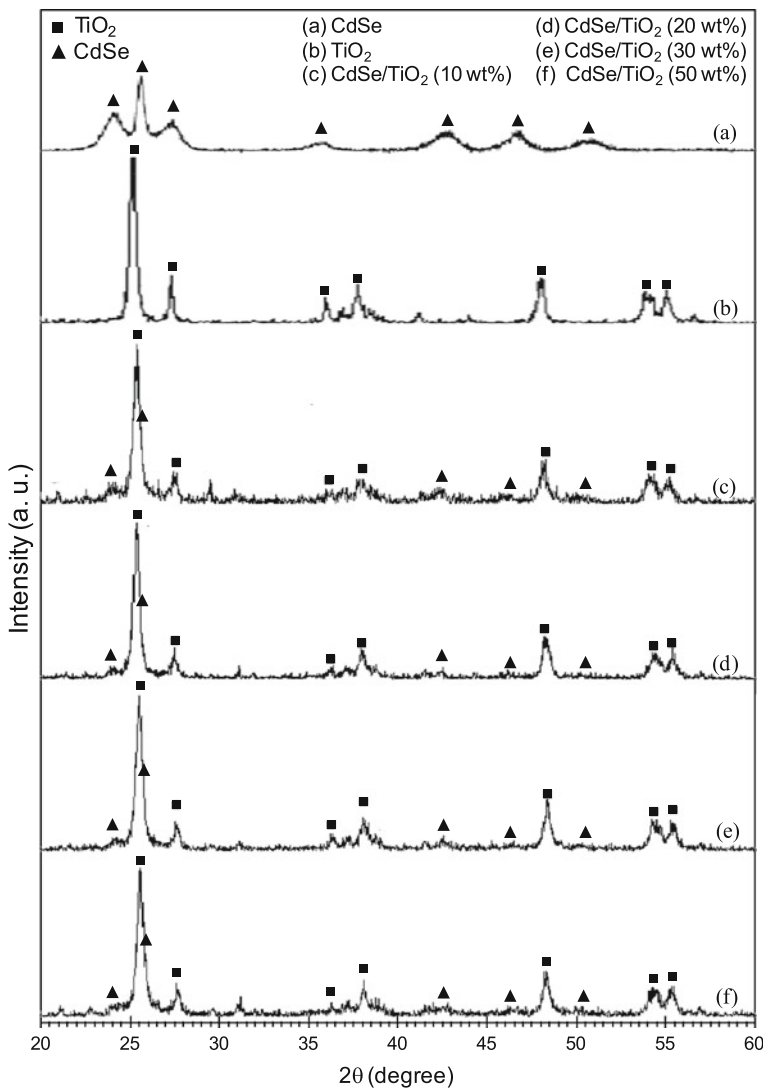


Fig. 3 XRD patterns of CdSe (a), non-modified TiO_2 (b), synthesized nanocatalysts: CdSe/TiO_2 (10 wt%) (c), CdSe/TiO_2 (20 wt%) (d), CdSe/TiO_2 (30 wt%) (e), and CdSe/TiO_2 (50 wt%) (f)

with a high degree of aggregation. The micrographs show a finer size distribution for synthesized nanocatalysts compared with that of TiO_2 nanoparticles. The BET analysis demonstrated 70 and $49 \text{ m}^2/\text{g}$ for CdSe/TiO_2 (20 wt%) and commercial Degussa TiO_2 , revealing more surface area available when incorporated with CdSe. This result is confirmed by the micrographs clearly showing the CdSe deposited on the TiO_2 nanoparticles with finer particle distribution.

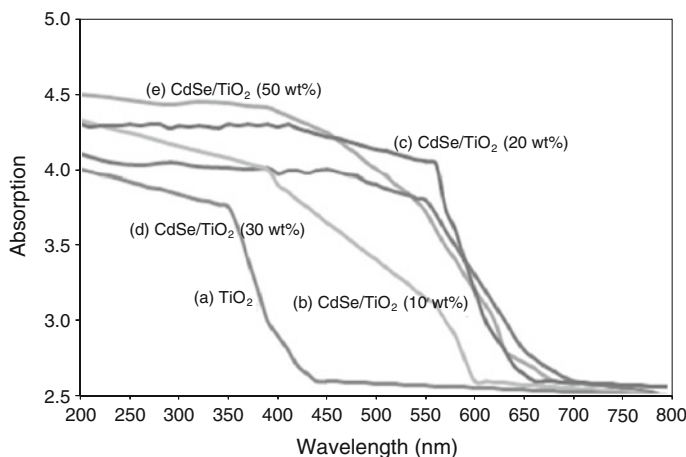


Fig. 4 UV-vis spectrum of non-modified TiO_2 (a), synthesized nanocatalysts: CdSe/TiO_2 (10 wt%) (b), CdSe/TiO_2 (20 wt%) (c), CdSe/TiO_2 (30 wt%) (d), and CdSe/TiO_2 (50 wt%) (e)

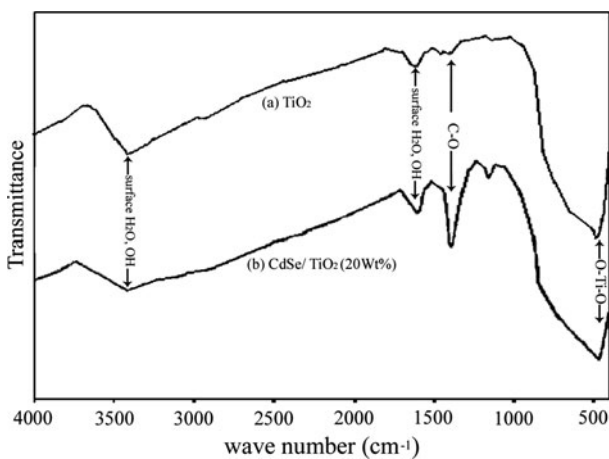


Fig. 5 FTIR spectra of non-modified TiO_2 (a) and synthesized nanocatalyst CdSe/TiO_2 (20 wt%) (b)

Photocatalytic activity

Phenol decomposition was carried out for measuring the photocatalytic activity of the synthesized nanocatalysts. Fig. 7 shows the decomposition of phenol under illumination of sunlight in the presence of the synthesized nanocatalysts compared to non-modified TiO_2 . The phenol residue percent was calculated using Eq. 5 and plotted versus time for comparison.

$$\text{Phenol residue (\%)} = \left(\frac{C}{C_o} \right) \times 100 \quad (5)$$

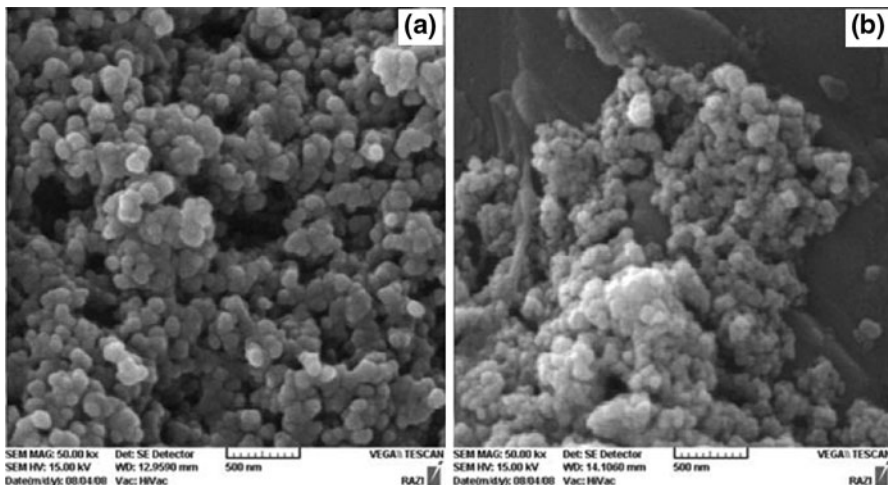


Fig. 6 SEM images of non-modified TiO_2 (a) and synthesized nanocatalyst CdSe/TiO_2 (20 wt%) (b)

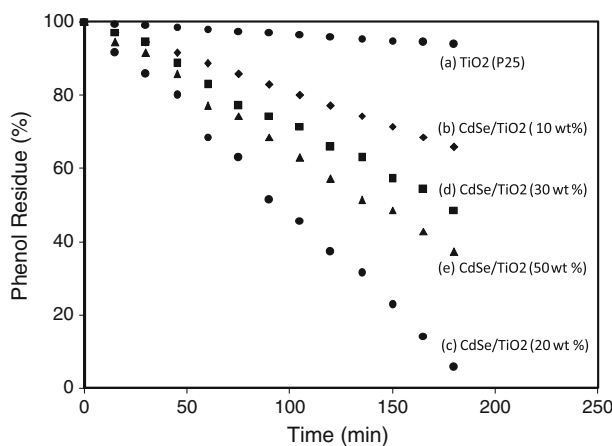


Fig. 7 Phenol decomposition under sunlight irradiation using non-modified TiO_2 (a) and synthesized nanocatalysts: CdSe/TiO_2 (10 wt%) (b), CdSe/TiO_2 (20 wt%) (c), CdSe/TiO_2 (30 wt%) (d), and CdSe/TiO_2 (50 wt%) (e)

Here C_0 is the initial total organic carbon and C is the total organic carbon at time t .

The results show that the synthesized CdSe/TiO_2 has a positive effect on the photocatalytic activity compared to that of commercial TiO_2 . The nanocatalyst with 20 wt% CdSe showed the best photocatalytic activity, decomposing 95% of phenol in 180 min while TiO_2 did not show any significant photocatalytic activity under the same condition. This result is in agreement with the results obtained using the UV-vis spectroscopy analysis.

The synthesized nanocatalyst has an absorption range in the visible spectrum making better use of the sunlight for electron generation, while that of the metal oxide only takes advantage of 10% of the sunlight spectrum in the UV range. The lowering in the band gap energy from 3.1 to 2.0 eV for the commercially available TiO_2 and that of the synthesized nanocatalyst (20 wt%) also justifies the profound photocatalytic properties. The synthesized nanocatalysts are sensitized to the visible light spectrum when incorporated with CdSe generating electron-holes. The generated electrons originally produced in the CdSe media find their way towards the Ti^{3+} sites on the TiO_2 nanoparticles providing an efficient charge separation. The generated electrons are scavenged by the oxygen molecules in the water medium producing hydroxyl radicals responsible for decomposition of the organic pollutant.

The results have shown that the incorporated CdSe has an optimum level (20 wt%) and less efficient nanocatalysts are obtained beyond and below this level. The results obtained from the photocatalytical studies suggest that in less CdSe content (10 wt%) less light is scavenged and less electron-holes are generated compared to that observed from the optimum condition (20 wt%) as observed in the UV-vis absorption studies. However, at higher CdSe contents (30 and 50 wt%) the generated electrons in the CdSe media are not efficiently devoted to available sites on the surface of the TiO_2 nanoparticles as a result of high degree of TiO_2 surface coverage by the CdSe. The generated electrons are suggested to recombine with the generated holes in either the CdSe or TiO_2 media.

Greater specific surface area as a result of CdSe deposition on the TiO_2 nanoparticles observed by the SEM micrographs and BET analysis for the synthesized nanocatalysts can be other reasons for better performance of the CdSe/ TiO_2 nanocatalysts.

The total organic carbon (TOC) analysis and phenol decomposition performance of the synthesized nanocatalyst, CdSe/ TiO_2 (20 wt%), is shown in Fig. 8.

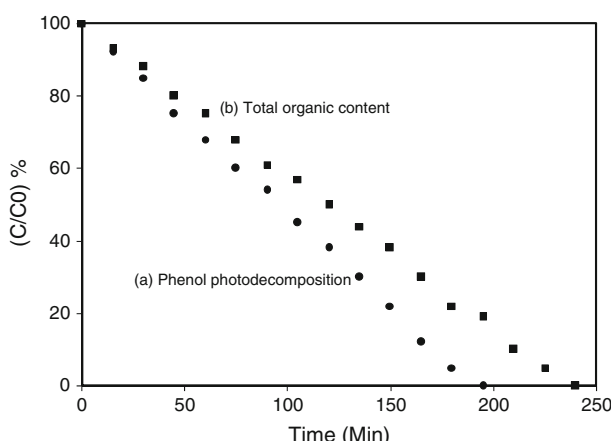


Fig. 8 TOC analysis (a) and phenol decomposition performance (b) of synthesized nanocatalyst: CdSe/ TiO_2 (20 wt%)

As can be indicated, a high concentration of organic carbon is present even after total phenol degradation (indicated by the UV-vis spectroscopy). This is due to the presence of other organic intermediates produced during the photodecomposition reactions, which is currently under investigation.

Conclusions

CdSe/TiO₂ nanocatalyst was prepared using ultrasonic approach. The photodecomposition efficiency of the catalyst was compared with that of commercial Degussa TiO₂ under sunlight irradiation where phenol was used as the organic pollutant. Nanocatalyst characterization revealed that the ultrasonic approach affects not only the crystal structure of the synthesized nanocatalyst but also the nanoparticle size. No significant photodecomposition was observed from the commercial Degussa TiO₂ under sunlight irradiation due to its UV limited absorption spectrum. The synthesized sample containing 20 w% CdSe proves to be the best candidate for photodecomposition of phenol in the ranges studied in this research. CdSe/TiO₂ has shown significant photodecomposition activity which can be explained by the shift in the absorption spectrum from the UV range to the visible range.

Acknowledgments The authors gratefully acknowledge Sahand University of Technology for the financial support of the project as well as Iran Nanotechnology Initiative Council for complementary financial support. They also wish to thank Mr. Jafarizad for the technical aid at analytical lab of Chemical Engineering Faculty.

References

1. Zhang J-C, Gao L-L, Cao W-L (2003) A study on the preparation and photocatalytic properties of TiO₂-SiO₂ nanocomposite photocatalyst by supercritical fluid drying. *Chin J Inorg Chem* 19:934–940
2. Ksibi M, Zemzemi A, Boukchina R (2003) Photocatalytic degradability of substituted phenols over UV irradiated TiO₂. *J Photochem Photobiol A* 159(1):61–70
3. Guo Z, Ma R, Li G (2006) Degradation of phenol by nanomaterial TiO₂ in wastewater. *Chem Eng J* 119(1):55–59
4. Han W, Zhu W, Zhang P, Zhang Y, Li L (2004) Photocatalytic degradation of phenols in aqueous solution under irradiation of 254 and 185 nm UV light. *Catal Today* 90(3–4):319–324
5. Wei T-Y, Wan C-c (1992) Kinetics of photocatalytic oxidation of phenol on TiO₂ surface. *J Photochem Photobiol A* 69(2):241–249
6. Ho W, Yu JC (2006) Sonochemical synthesis and visible light photocatalytic behavior of CdSe and CdSe/TiO₂ nanoparticles. *J Mol Catal A* 247(1–2):268–274
7. Qi X-H, Wang Z-H, Zhuang Y-Y, Yu Y, Li J-I (2005) Study on the photocatalysis performance and degradation kinetics of X-3B over modified titanium dioxide. *J Hazard Mater* 118(1–3):219–225
8. Szabó-Bárdos E, Pétervári E, El-Zein V, Horváth A (2006) Photocatalytic decomposition of aspartic acid over bare and silver deposited TiO₂. *J Photochem Photobiol A* 184(1–2):221–227
9. Yan X, He J, Evans DG, Zhu Y, Duan X (2004) Preparation, characterization and photocatalytic activity of TiO₂ formed from a mesoporous precursor. *J Porous Mater* 11(3):131–140
10. Khodja AA, Sehili T, Pilichowski J-F, Boule P (2001) Photocatalytic degradation of 2-phenylphenol on TiO₂ and ZnO in aqueous suspensions. *J Photochem Photobiol A* 141(2–3):231–239
11. Ku Y, Leu R-M, Lee K-C (1996) Decomposition of 2-chlorophenol in aqueous solution by UV irradiation with the presence of titanium dioxide. *Water Res* 30(11):2569–2578

12. Theurich J, Lindner M, Bahnemann DW (1996) Photocatalytic degradation of 4-chlorophenol in aerated aqueous titanium dioxide suspension: a kinetic and mechanistic study. *Langmuir* 12: 6368–6376
13. Bacsa RR, Kiwi J (1998) Effect of rutile phase on the photocatalytic properties of nanocrystalline titania during the degradation of *p*-coumaric acid. *Appl Catal B* 16(1):19–29
14. Mane RS, Roh SJ, Joo O-S, Lokhande CD, Han S-H (2005) Improved performance of dense TiO₂/CdSe coupled thin films by low temperature process. *Electrochim Acta* 50(12):2453–2459
15. Lo S-C, Lin C-F, Wu C-H, Hsieh P-H (2004) Capability of coupled CdSe/TiO₂ for photocatalytic degradation of 4-chlorophenol. *J Hazard Mater* 114(1–3):183–190
16. Linsebigler AL, Lu G, Yates JT (1995) Photocatalysis on TiO₂ surfaces: principles, mechanisms, and selected results. *Chem Rev* 95(3):735–758
17. Ding Z, Lu GQ, Greenfield PF (2000) Role of the crystallite phase of TiO₂ in heterogeneous photocatalysis for phenol oxidation in water. *J Phys Chem B* 104(19):4815–4820. doi:[10.1021/jp993819b](https://doi.org/10.1021/jp993819b)
18. Kolen'ko YV, Garshev AV, Churagulov BR, Boujday S, Portes P, Colbeau-Justin C (2005) Photocatalytic activity of sol–gel derived titania converted into nanocrystalline powders by supercritical drying. *J Photochem Photobiol A* 172(1):19–26
19. Deng C, James FP, Wright VP (1998) Poly(tetraethylene glycol malonate)–titanium oxide hybrid materials by sol–gel methods. *J Mater Chem* 8(1):153–159
20. Zheng M, Gu M, Jin Y, Jin G (2000) Preparation, structure and properties of TiO₂–PVP hybrid films. *Mater Sci Eng B* 77(1):55–59